

# The formation of massive stars: accretion, disks, and the development of hypercompact HII regions

Eric Keto

*Harvard-Smithsonian Center for Astrophysics, 60 Garden St., Cambridge, MA 02138*

## ABSTRACT

The hypothesis that massive stars form by accretion can be investigated by simple analytical calculations that describe the effect that the formation of a massive star has on its own accretion flow. Within a simple accretion model that includes angular momentum, that of gas flow on ballistic trajectories around a star, the increasing ionization of a massive star growing by accretion produces a three-stage evolutionary sequence. The ionization first forms a small quasi-spherical HII region gravitationally trapped within the accretion flow. At this stage the flow of ionized gas is entirely inward. As the ionization increases, the HII region transitions to a bipolar morphology in which the inflow is replaced by outflow within a narrow range of angle with about the bipolar axis. At higher rates of ionization, the opening angle of the outflow region progressively increases. Eventually, in the third stage, the accretion is confined to a thin region about an equatorial disk. Throughout this early evolution, the HII region is of hypercompact to ultracompact size depending on the mass of the enclosed star or stars. These small HII regions whose dynamics are dominated by stellar gravitation and accretion are different than compact and larger HII regions whose dynamics are dominated by the thermal pressure of the ionized gas.

*Subject headings:* stars: early type — stars: formation — ISM: HII regions

## 1. Introduction

The hypothesis that massive stars form by accretion can be investigated by simple analytical calculations that describe the effect that the formation of a massive star has on its own accretion flow. An earlier paper (Keto 2002b) studied the effect of star formation in a spherically-symmetric, steady-state flow (Bondi 1952) and showed how a molecular

accretion flow may pass through an ionization front and continue toward the star as an ionized accretion flow. In this case, the HII region is the ionized inner zone of a continuous two-phase accretion flow. More generally, angular momentum in an accretion flow will result in a flattened geometry with different consequences for the structure of the ionized accretion flow and HII region.

This paper investigates the effects of the ionizing radiation of a massive star on an accretion flow with angular momentum, modeled as gas flow on ballistic trajectories around a star (Ulrich 1976). The model is described by a few parameters: the gas density in the flow, the angular momentum, the mass of the star, and the flux of ionizing radiation. Alternatively, the model can be described in terms of three characteristic radii: characteristic radii,  $R_i$ , the radius of ionization equilibrium,  $R_b$ , the radius where the escape velocity equals the sound speed, and  $R_d$ , the radius of disk formation where the gravitational and centrifugal forces balance,

Models with different ratios of these three radii produce HII regions with different morphologies and dynamics. In particular, increasing the ratio  $R_i/R_b$  radius of ionization results in a progression of HII regions from quasi-spherical, gravitationally-trapped Keto (2002b, 2003) through bipolar to a final morphology similar to that around a photo-evaporating disk as described by Hollenbach et al. (1994), Yorke (1995), Yorke & Welz (1996), Lizano et al. (1996), Johnstone, Hollenbach, & Bally (1998), and Lugo, Lizano & Garay (2004). This progression suggests an evolutionary sequence for an HII region around a star that is growing by accretion. As the star gains mass, the location of the radius,  $R_b$ , will increase proportionally with the mass of the star. The radius of ionization equilibrium,  $R_i$ , will also increase but as a higher power of the mass because the flux of ionizing radiation depends on the temperature of the star. Thus this simple model of ionization within an accretion flow provides an understanding of the relationship between the several different observed HII region morphologies on the hypercompact and ultracompact scales.

## 2. Relevant results from the spherical model: the 3 evolutionary stages of an HII region

Stellar structure models suggest that massive stars that form by contraction have a shorter pre-main sequence phase (PMS) than low mass stars, and that massive stars that form by accretion have no PMS phase at all because massive stars begin hydrogen burning while still accreting (Palla & Stahler 1993; Beech & Mitalas 1994; Chieffi, Staniero & Salaris 1995; Bernasconi & Maeder 1996; Behrend & Maeder 2001; Norberg & Maeder 2000; Keto 2003). These calculations suggest that a massive star that is forming by accretion will reach the

main sequence with a mass below that which would produce sufficient ionizing radiation to maintain an HII region around the star. The non-existent HII region at this stage may be described as *quenched* (Walmsley 1995). Because the production of ionizing photons increases as a higher power of the stellar mass than does the accretion rate, eventually the flux of ionizing radiation,  $J_*$ , from a star that is gaining mass by accretion, will exceed the flux of neutral gas onto the star (Keto 2003),

$$J_* > 4\pi r_*^2 n_H v \quad (1)$$

where  $r_*$  is the stellar radius,  $n_H$  is the the number density of neutral gas, and  $v$  the inflow velocity.

If the density of the accretion flow decreases with distance no faster than  $r^{-3/2}$ , then the HII region that develops in the flow will be bounded at a distance,  $R_i$  (Franco, Tenorio-Tagle & Bodenheimer 1990), defined by the balance of the ionizations and recombinations (Spitzer 1978, eqn. 5.20),

$$J_* - \int_{r_*}^{R_i} 4\pi r^2 n_e^2(r) \alpha^2 dr = 0 \quad (2)$$

This equation incorporates the "on-the-spot" approximation with  $\alpha$  the recombination rate to all Rydberg levels of H above the first level,  $n = 1$ .

The small HII region that develops just as the quenched phase (equation 1) ends cannot expand hydrodynamically because the outward pressure of the ionized gas is less than the inward gravitational force of the star. Instead, the ionized gas forms part of a continuous accretion flow with an outer molecular phase and an inner ionized phase separated by a static ionization front within the flow. The HII region, which at this stage is the inner part of the accretion flow, may be described as *gravitationally trapped* (Keto 2002b, 2003). As the star continues to gain mass and its flux of ionizing radiation increases, the boundary of the HII region, whose location is determined by ionization equilibrium rather than pressure balance, will be found at greater radii. Once a radius is reached where the escape velocity from the star is below the sound speed of the ionized gas, the HII region will begin to expand hydrodynamically. This radius is approximately equal to the Bondi-Parker trans-sonic radius where the velocity of the incoming accretion flow first reaches the sound speed of the ionized gas,

$$R_b = GM_*/2c^2 \quad (3)$$

where  $M_*$  is the mass of the star and  $c$  is the sound speed. The evolution of the HII region then transitions to a phase of *pressure-driven expansion* in which the gravitational attraction of the star is negligible over most of the HII region. These pressure dominated HII regions are adequately described by models with no gravitational force (Spitzer 1978; Dyson & Williams

1980; Shu 1992). The model for the development of an HII region within a spherical accretion flow thus suggests three stages: 1) quenched or non-existent, 2) gravitationally trapped, and 3) pressure driven-expansion. The divisions between the stages occur when the radius of ionization equilibrium,  $R_i$ , (equation 2).

### 3. A non-spherical accretion flow

One simple model of accretion that includes rotation equates the streamlines of an accretion flow with ballistic trajectories around a point mass (Ulrich 1976; Cassen & Moosman 1981; Chevalier 1983; Terebey, Shu & Cassen 1984) The flow is determined by the gravitational attraction of the point source subject to conservation of angular momentum and mass. In particular, the model ignores the pressure and self-gravity of the gas. The initial distribution of angular momentum is that of solid body rotation on an arbitrary radius or conceptual spherical surface some distance from the star. Thus on each trajectory, the specific angular momentum,  $\Gamma \propto \sin \theta_0$ , where  $\theta_0$  is the initial polar angle. The gas density is described by the conservation of mass along streamlines. In this model, an accretion disk develops as the gas density increases along inwardly converging streamlines flattened by the angular momentum of the flow. A limitation of the model is that the mid-plane density is not defined whereas a more complete model would describe the density across the mid-plane as a pressure supported disk (Shakura & Sunyaev 1973; Lynden-Bell & Pringle 1974; Pringle 1981; Hartmann 1998; Whitney et al. 2003). This deficiency may be ignored if, as in the examples that follow, the scale of the HII region developed within this accretion flow is larger than the scale height of the disk (see §6). The equations for the velocity and density at a position  $(r, \theta)$  are (Ulrich 1976),

$$v_r = -\left(\frac{GM}{r}\right)^{1/2} \left(1 + \frac{\cos \theta}{\cos \theta_0}\right)^{1/2} \quad (4)$$

$$v_\theta = \left(\frac{GM}{r}\right)^{1/2} (\cos \theta_0 - \cos \theta) \left(1 + \frac{\cos \theta_0 + \cos \theta}{\cos \theta_0 \sin \theta}\right)^{1/2} \quad (5)$$

$$v_\phi = \left(\frac{GM}{r}\right)^{1/2} \frac{\sin \theta_0}{\sin \theta} \left(1 + \frac{\cos \theta}{\cos \theta_0}\right)^{1/2} \quad (6)$$

where,

$$r = \frac{R_d \cos \theta_0 \sin \theta_0^2}{\cos \theta_0 - \cos \theta} \quad (7)$$

This last equation includes the parameter,  $R_d$ , which is the radius at which the gravitational force equals the centrifugal force in the mid-plane,

$$\Gamma^2/r_d^3 = GM/r_d^2 \quad (8)$$

This radius, approximately where the accretion flow transitions from a quasi-spherical inflow to a rotationally supported disk, may also be written in a form analogous to the Bondi-Parker transonic radius as,

$$R_d = GM/v_k^2 \quad (9)$$

where  $v_k$ , the orbital velocity at  $R_d$ , replaces the sound speed in equation 3. The gas density from mass conservation is (Mendoza, Canto, Raga 2004),

$$n = n_0 r^{-3/2} \left(1 + \frac{\cos \theta}{\cos \theta_0}\right)^{-1/2} (1 + r^{-1}(3 \cos^2 \theta_0 - 1))^{-1} \quad (10)$$

where the number density,  $n_0$ , is defined through the mass density,  $\mu n_0$ , by the mass accretion rate,

$$\dot{M} = \mu n_0 4\pi R_d^2 v_k \quad (11)$$

#### 4. The development of an HII region in the non-spherical accretion flow

An HII region will develop at the center of the flow defined by equations 4 through 11 once the ionizing flux of the accreting star satisfies the condition in equation 1. However, in a non-spherical flow, the gas density is not radially symmetric, and therefore the HII boundary,  $R_i$ , is at larger distances in directions where the gas density is lower. In the axially symmetric model above, the boundary is therefore a function of the polar angle,  $\theta$ . The spherical model of §2 suggests that if  $R_i > R_b$  the HII region expands hydrodynamically. Thus while somewhat idealized, in the non-spherical model the HII region may be expanding over a range of angle  $\theta$  about the polar axis while the accretion flow continues to flow into and through the HII in a different range of angle  $\theta$  around the plane of the disk.

This simple model of the ionization of an accretion flow does not explicitly include the effect of a stellar wind on the HII region. We know that unembedded early-type stars produce powerful winds that at their terminal velocities have mechanical energies,  $\rho v_t^2$ , that exceed the mechanical energies of star-forming accretion flows (Lamers & Cassinelli 1999). However, because the winds accelerate off the surface of the star the wind energy is negligible near the star and, in the idealized spherical model, the wind may be suppressed by the accretion flow. Once inflow ends because the gas within the HII region begins expanding ( $R_i > R_b$ ), the wind may be expected to break out and dominate the hydrodynamics. Thus in the non-spherical model, the following approximation is adopted. At a polar angle,  $\theta$ , where  $R_i(\theta) > R_b$ , the inflow is replaced by the simplest model of a stellar wind (Parker 1958). This wind solution is the analogue of the Bondi accretion flow and described by the same equation,

$$\frac{d}{dr} \left( \frac{v^2}{2} \right) + \frac{dP}{dr} + \frac{GM}{r^2} = 0 \quad (12)$$

but with the boundary conditions that the flow is subsonic at the stellar surface and supersonic beyond the transonic radius. In the case of non-spherical flows, the location of the transonic radius depends on the geometry of the flow, specifically on the divergence of the streamlines about the star (Kopp & Holzer 1976). However, if the divergence is approximately spherical, the transonic point will be approximately located by equation 3. For simplicity, this approximation is adopted. The resulting model of a wind in the polar directions and accretion at lower latitudes is inconsistent in that the wind solution is driven by hydrodynamic pressure, but pressure is neglected in the accretion flow. Nonetheless, the examples in §6 will show that this approximation is useful on a conceptual level and produces models that describe the morphology of observed HII regions. Different models that describe the interaction of a wind and accretion flow include Wilkin & Stahler (1998), Mendoza, Canto, Raga (2004), and Cunningham et al. (2005).

### 5. The 3 R's of hypercompact HII regions

The equations in sections §2 and §4 fully describe the model of an HII region in a non-spherical accretion flow. The morphology of the HII region depends on a few physical quantities that are specified as parameters of the model: the gas density and angular momentum in the accretion flow, and the mass and flux of ionizing radiation of the star. Because these physical quantities have different units, it is helpful to organize them into parameters of the same physical dimension as 3 characteristic radii. The radius of disk formation,  $R_d$  (equation 9), along with the Bondi-Parker radius,  $R_b$  (equation 3), and the radius of ionization equilibrium,  $R_i$  (equation 2), may be called the 3 R's of HII regions in that they describe the basic structure of the accretion flow and HII region.

We may also combine these 3 characteristic radii into non-dimensional ratios, for example  $R_i/R_d$ ,  $R_i/R_b$ ,  $R_d/R_b$  to see that the models are scale-free, and that it is the relative magnitudes of the 3 radii that are important in describing the structure of the accretion flows and HII regions. Thus a model appropriate for a common accretion flow onto several O stars such as in G10.6-0.4 with a total stellar mass of a few hundred  $M_\odot$  (Keto & Wood 2006) may have the same structure as a model for a single B star such as IRAS20126 (Cesaroni et al. 1997, 1999) provided that the three ratios are the same.

Because the model structures depend on only 3 characteristic radii or 3 ratios, then only a few model examples are required to illustrate the possible variations as well as suggest an evolutionary sequence for HII regions. So that these models may be more easily related to the densities and stellar types familiar from observations of high mass star forming regions, the examples in the next section are presented in units appropriate for early B stars and late

O stars since these are most commonly observed massive stars. These models are applicable, if scaled up, to accretion flows as large as those onto groups of early O stars such as G10.6-0.4 (Keto & Wood 2006).

## 6. Examples and evolution

### 6.1. Ionization

The first example illustrates the effect of increasing the ionizing flux within the same accretion flow. This comparison illustrates the differences as  $R_i/R_b$  is greater than, approximately equal to, or less than one. (In this example for the purpose of this comparison, we set  $R_d \approx R_b$ .) As the ionizing radiation from the star increases, and  $R_i$  increases relative to  $R_b$ , the HII region transitions through three phases from nearly spherical inflow of the ionized gas through bipolar to nearly spherical outflow.

The initial model is composed of a B1 star with a mass of  $18 M_\odot$  and a flux of ionizing radiation of  $10^{45}$  photons  $s^{-1}$  (Vacca, Garmany & Shull 1996) within an accretion flow with  $R_d = 42$  AU ( $\Gamma_0 = 0.04$  kms $^{-1}$  pc),  $R_b = 43$  AU, and a gas density,  $n_0$  of  $10^7$  cm $^{-3}$ . The mass accretion rate (equation 11) is  $6 \times 10^{-6} M_\odot$  yr $^{-1}$ . Stellar structure calculations suggest that this accretion rate is near the minimum required for the formation of stars of this mass (Keto 2003; Keto & Wood 2006). Higher rates might be required to form stars of higher mass.

Figure 1 (*top*) shows that at this flux level and density, although the HII region has a slightly bipolar shape owing to the flattening of the flow, the boundary of the HII region is entirely within the Bondi-Parker critical radius ( $R_i < R_b$  at all polar angles). Thus the HII region is trapped within the gravitational field of the star, and accretion may proceed through the HII region at all angles.

Increasing the stellar mass to  $20 M_\odot$  and the flux of ionizing radiation to  $7 \times 10^{45}$  photons  $s^{-1}$ , corresponding to an B0.5 star, increases the extent of the ionization sufficiently so that  $R_i \geq R_b$  in a narrow range of angle about the bipolar axis. Within this angular range, we assume that the HII region begins to expand and the structure and dynamics are described by an outflow or wind driven by the thermal pressure of the ionized gas. Accretion through the HII region continues at lower latitudes (figure 1 *middle*).

Increasing the stellar mass to  $22 M_\odot$  and the flux of ionizing radiation to  $10^{47}$  photons  $s^{-1}$ , corresponding to an O9 star, results in a model with  $R_i > R_b$ , and thus outflow, everywhere except at a narrow range of angle just around the disk (figure 1 *bottom*). This

third-stage structure is similar to the photo-evaporating disk model (Hollenbach et al. 1994; Yorke 1995; Yorke & Welz 1996; Lizano et al. 1996; Johnstone, Hollenbach, & Bally 1998; Lugo, Lizano & Garay 2004) except that here the outflow is radially from the center of the HII region rather than vertically off a disk. A more complete model would include the evaporation off the disk in the outflow.

In this scenario, the bipolar phase is relatively brief in the evolution between the gravitationally trapped and outflow phases. In this example, the bipolar phase corresponds to a range of stellar mass between 20 and 22  $M_{\odot}$ .

## 6.2. Angular momentum

The second example shows the effect of different values of the angular momentum on the structure of the accretion flow. This example illustrates the difference as  $R_b/R_d$  is greater or less than one. Flows that have relatively low angular momentum will produce what may be described as a fat accretion torus around a growing star while those with relatively high angular momentum will produce a thin disk. Because the density of the flow increases inward following mass conservation regardless of the angular momentum, the difference between the two cases relates to where in the flow the gas density becomes observationally significant with respect to the flattening of the flow. The flow becomes observable as the gas density approaches the critical density for collisional de-excitation,  $n_c = A_{ij}/C_{ij}$ , where  $A_{ij}$  is the Einstein A coefficient ( $\text{sec}^{-1}$ ) and  $C_{ij}$  is the collision rate ( $\text{cm}^{-3} \text{sec}^{-1}$ ) for the particular molecular tracer employed in an observation. In a model with low angular momentum, the gas will reach the critical density before flattening into a disk, and the molecular accretion flow will be detected as a quasi-spherical rotating flow or fat torus. In the high angular momentum case, the flow will form a disk before the gas density in the surrounding flow exceeds the critical density. In this case the observations will tend to see the flattened disk.

Figure 2 shows two variations of the same model. Both models include a star of 20  $M_{\odot}$  and flux of ionizing radiation of  $3 \times 10^{46}$  photons  $\text{s}^{-1}$  corresponding to type B0 – O9.5. At this mass,  $R_b = 54$  AU. In one model, the angular momentum is  $\Gamma_0 = 0.04$   $\text{kms}^{-1}$  pc, while in the second model the rotation rate is 2 times higher. The values of  $R_d$  are therefore 38 AU and 152 AU respectively. Because of the greater inward increase in the gas density in the flattened, high-angular-momentum flow, the density in this flow is set lower,  $n_0 = 1 \times 10^6 \text{ cm}^{-3}$ , rather than  $n_0 = 3 \times 10^7 \text{ cm}^{-3}$ , so that similar densities are maintained at the center of the flow, and therefore, similar opening angles for the bipolar outflow. The mass accretion rates for each model are  $6.6 \times 10^{-6}$  and  $1.8 \times 10^{-5} M_{\odot} \text{ yr}^{-1}$ . The two density distributions shown in figure 2 suggest that accretion disks and "fat toroids" may be different



expressions of the same model accretion flow with different values of the angular momentum or equivalently different values of  $R_d$  with respect to  $R_b$ .

### 6.3. Limitations of the model

The model of accretion on ballistic trajectories in section §3 does not include pressure forces and therefore does not describe a pressure supported disk at the mid-plane. The density in such a disk could potentially affect the morphology of an HII region depending on the structure of the disk. Little is known either observationally or theoretically about disks around massive stars. If these disks are similar to those around low mass stars, then we can calculate how a scaled-up, low-mass disk would affect the HII region morphologies in the examples above. To do this we add to the model accretion flows in the examples above the density of a disk described as (Whitney et al. 2003, equation 3),

$$\rho(r) = \rho_0 \left(1 - \sqrt{\frac{R_*}{r}}\right) \left(\frac{R_*}{r}\right)^\alpha \exp \left[ -\frac{1}{2} \left(\frac{z}{H(r)}\right)^2 \right] \quad (13)$$

where  $r$  is the radius in the disk mid-plane,  $z$  is the height above the plane,  $\alpha = 2.25$ , and the scale height,  $H(r) = H_0(r/R_*)^\beta$  with  $H_0 = 0.1R_*$  (AU) and  $\beta = 1.25$ . The density,  $\rho_0$  is defined by the assumption that the total mass of the disk within  $R_d$  is  $0.1M_*$ . These additional calculations (not shown) demonstrate that the inclusion of such a disk does not affect the morphologies of the HII regions in these examples. This is because the scale height of the pressure-supported disk at the radii where the boundary of the HII region meets the mid-plane is small compared to the thickness of the "disk" created by the flattening of the accretion flow. Because this pressure-supported disk is an arbitrary addition to the model that does not affect the results sought in this investigation, this disk is not considered further.

## 7. The importance of stellar gravity and accretion on Hypercompacts and small Ultracomacts

The morphologies produced by models of HII regions that develop within accretion flows are potentially quite varied and match many of the observed morphologies, particularly those observed at the smallest scales. In particular, the bipolar HII regions are predominantly a small scale phenomenon. For example, there is no classification for bipolar morphology in the Wood & Churchwell (1989) and Kurtz et al. (1994) survey of ultracompact HII regions whereas Depree et al. (2005) find it necessary to introduce this class to describe the morphologies of hypercompact HII regions.

The size scale,  $\sim 0.01$  pc (2000 AU), of a large hypercompact or small ultracompact HII region (Kurtz 2000), is about 20 times the radius,  $R_b$  around a single massive star. What then is the relevance of the stellar gravity for most observed HC and UC HII regions?

First, O stars do not appear to form alone, but in small groups or clusters of early type stars that may also contain some number of lower mass stars. The radius,  $R_b$ , scales with the attracting mass. Groups or small clusters of stars with a few hundred  $M_\odot$  contained within a common HII region are suggested by observations of a few of the brightest HII regions that show molecular or ionized accretion on scales of  $10^3$  AU (Zhang & Ho 1997; Young, Keto & Ho 1998; Keto 2002a; Sollins et al. 2005; Keto & Wood 2006). Thus the gravity of groups or small clusters may be significant even on the size scales of ultracompact HII regions.

Second, the HII region need not be strictly smaller than  $R_b$  for the stellar gravitational attraction to affect its structure. For example, if the HII region is in effect an expanding wind, as in the model shown in figure 1 (*bottom*), then because the wind solution is quasi-hydrostatic (Keto 2003, equation 4) inside of  $R_b$ , the HII region will be quite dense within this radius even though the boundary,  $R_i > R_b$ . Outside of  $R_b$ , mass conservation within the converging accretion flow and within the diverging outflow generally requires that the flows have density gradients. Thus even beyond  $R_b$ , in the region dominated by pressure forces, the density is not uniform. High frequency observations would show a bright core whereas low frequency observations of the same HII region would show surrounding low-level extended emission.

## 8. Jets, outflows and disks

The outflows described here are simple models of stellar winds driven by the pressure of the ionized gas (Parker isothermal wind (Parker 1958)) in the HII region and confined in a specific way defined by the ratio of  $R_i/R_b$  as a function of angle, but nonetheless essentially by the geometry of the surrounding accretion flow. Thus these outflows require both significant ionizing flux from the star and a massive accretion flow. In this respect they are quite different from the more familiar bipolar jets or outflows associated with young low-mass stars. These latter are not completely understood, but are thought to be driven by the twisting of magnetic fields by a thin accretion disk. Although this paper has not dealt with magnetically-driven outflows, these are not incompatible with the HII-driven outflows. The hypothesis of massive star formation presented here, following Keto (2002b, 2003), suggests that both occur. In this hypothesis, high mass stars grow by accretion from lower mass stars. Since magnetically-driven outflows are an inescapable part of low-mass star formation, the

massive stars-to-be must reach spectral type B with a magnetically-driven outflow.

As the star continues to grow to earlier type B, and the ionizing radiation creates an HII region, what becomes of the magnetically driven outflow? Beuther & Shepherd (2005) suggest that there is a lack of observations of collimated jet-like outflows associated with stars earlier than type B1 compared with the number of observations of jet-like outflows from later type B stars. At the moment we do not know whether the jets are destroyed by processes associated with the ionization or survive the formation of the HII region (Tan & McKee 2003) but are difficult to detect.

## 9. Comparison with observations

A model of accretion with a bipolar ionized outflow has been compared to observations of both ionized gas and molecular gas in and around the ultracompact HII region G10.6-0.4 (Keto & Wood 2006). The model for the accretion flow in G10.6-0.4 is based on the same model of streamlines on ballistic trajectories presented here. These observations are unique in mapping the velocities in both the molecular and ionized gas and in following the accretion flow from the molecular phase through the ionized phase. However, the source G10.6-0.4 is not unique. Molecular line observations of G28.20-0.05 (Sollins et al. 2005) and G24.78+0.08 (Beltran et al. 2006) have also been interpreted as accretion disks and outflows. Other observations that report disks or torii around massive stars, some with associated outflows include (Cesaroni et al. 1997; Hofner et al. 1999; Cesaroni et al. 1999; Shepherd & Kurtz 1999; Shepherd, Claussen & Kurtz 2001; Beltran et al. 2004, 2005; Zhang et al. 1998, 2002; Kumar et al. 2003; Chini et al. 2004; Beuther et al. 2004; Patel et al. 2005)

## 10. Conclusions

This paper provides a simple theoretical description of some of the effects of the ionization of a massive-star forming accretion flow. The model presented here is based on three simple models: (1) accretion with rotation as streamlines on ballistic trajectories (Ulrich 1976); (2) an outflow as a pressure-driven isothermal wind (Parker 1958); and (3) an ionization front gravitationally trapped within an accretion flow (Keto 2002b). The composite model applies to the evolutionary phase in the formation of massive stars of type B and earlier when the stars are both hot enough to ionize an HII region around the star and yet are still growing by accretion. The model accretion flows and HII regions may be described in terms of three characteristic radii which completely determine the morphology and flow

pattern. Variation of the relative magnitudes of the parameters suggests how different morphologies may be related to the same underlying model. The models further suggest an evolutionary sequence driven by the increasing ionization of a star growing by accretion. These hypercompact to ultracompact HII regions are different in that their dynamics are dominated by gravitational force of their stars whereas the larger HII regions are dominated by the thermal pressure of the ionized gas.

## REFERENCES

- Beech, M., & Mitalas, R., 1994, *ApJ Suppl.*, 95, 517
- Behrend, A. & Maeder, A., 2001, *AA*, 373, 190
- Bernasconi, P. & Maeder, A., 1996, *AA*, 307, 839
- Beltran, M. T., Cesaroni, R., Neri, R., Codella, C., Furuya, R. S., Testi, L. & Olmi, L. 2004, *ApJ*, 601, L187
- Beltran, M.T., Cesaroni, R., Neri, R., Codella, C., Furuya, R.S., Testi, L., Olmi, L., 2005, *AA*, 435, 901
- Beltran, M.T., Cesaroni, R., Codella, C., Testi, L., Furuya, R.S., Olmi, L., 2006, *Nature*, 443, 427
- Bondi, H., 1952, *MNRAS*, 112, 195
- Beuther, H.; Hunter, T. R.; Zhang, Q.; Sridharan, T. K.; Zhao, J.-H.; Sollins, P.; Ho, P. T. P.; Ohashi, N.; Su, Y. N.; Lim, J.; Liu, S.-Y., 2004, *ApJ*, 616, L23
- Beuther, H. & Shepherd, D., 2005, *Cores to Clusters Star Formation with Next Generation Telescopes*, *Astrophysics and Space Sciences Library*, vol 324, pg 105, eds: Kumar, M.S.N., Tafalla, M., Caselli, P., astro-ph/0504074
- Cassen, P. & Moosman, A., 1981, *Icarus*, 48, 353
- Cesaroni, R., Felli, M., Testi, L., Walmsley, C. M., Olmi, L., *AA*, 1997, 325, 725
- Cesaroni, R., Felli, M., Jenness, T., Neri, R., Olmi, L., Robberto, M., Testi, L., Walmsley, C. M., *AA*, 345, 949
- Chevalier, R.A., 1983, *ApJ*, 268, 753

- Chieffi, A., Staniero, O., & Salaris, M., 1995, *ApJ*, 445, L39
- Chini, R., Hoffmeister, V., Kimeswenger, S., Nielbock, M., Nurnberger, D., Schmidtobreick, L. & Sterzik, M., 2004, *Nature*, 429, 155
- Cunningham, A., Frank, A., Hartmann, L., 2005, *ApJ*, 631, 1010
- DePree, C.G., Wilner, D.J., Deblasio, J., Mercer, A.J., Davis, L.E., 2005, *ApJL*, 624, L101
- Dyson, J. & Williams, D.A., 1997, *The Physics of the Interstellar Medium*, Halsted: NY
- Hofner, P., Cesaroni, R., Rodriguez, L.F., Marti, J., 1999, 345, L43
- Franco, J., Tenorio-Tagle, G. & Bodenheimer, P., 1990, *ApJ*, 349, 126
- Hartmann, L., *Accretion Processes in Star Formation* (Cambridge: Cambridge Univ. Press)
- Hollenbach, D., Johnstone, D., Lizano, S., Shu, F., 1994, *ApJ*, 428, 654
- Johnstone, D., Hollenbach, D., & Bally, J., 1998, *ApJ*, 499, 758
- Keto, E., 2002a, *ApJ*, 568, 754
- Keto, E., 2002b, *ApJ*, 580, 980
- Keto, E., 2003, *ApJ*, 599, 1196
- Keto, E., Rybicki, G., Bergin, E.A., Plume, R., 2004, *ApJ*, 613,355
- Keto, E. & Wood, K., 2006, *ApJ*, 637, 850
- Kopp, R.A. & Holzer, T.E., 1976, *Solar Physics*, 49, 43
- Kumar, M., Fernandez, A., Hunter, T., Davis, C., Kurtz, S., 2003, *AA*, 412, 175
- Kurtz, S., Churchwell, E., Wood, D.O.S., 1994, *ApJS*, 91, 659
- Kurtz, S., 2000, *RevMexAA*, 9, 169
- Lamers, H. & Cassinelli, J., 1999, *Introduction to Stellar Winds*, Cambridge Univ. Press
- Lizano, S., Canto, J., Garay, G., Hollenbach, D., 1996, *ApJ*, 465, 216
- Lugo, J., Lizano, S., Garay, G., 2004, *ApJ*, 614, 807
- Lynden-Bell, D. & Pringle, J.E., 1974, 168, 603

- Pringle, J.E., 1981 ARAA, 19, 137
- Norberg, P. & Maeder, A., 2000, AA, 359, 1025
- Mendoza, S., Canto, J., Raga, A.C., 2004 Rev. Mex. AA, 40, 147
- Palla, F., & Stahler, S., 1993, ApJ, 418, 414
- Parker, E., 1958, ApJ, 128, 664
- Patel, N.A., Curiel, S., Sridharan, T.K., Zhang, Q., Hunter, T.R., Ho, P.T.P., Torrelles, J.M., Moran, J.M., Gomez, J.F., Anglada, G., 2005, Nature, 437, 109
- Shakura, N.I. & Sunyaev, R.A., 1973, A&A, 24, 337
- Shepherd, D. & Kurtz, S., 1999, ApJ, 523, 690
- Shepherd, D., Claussen, M., & Kurtz, S., 2001, Science, 292, 1513
- Shu, F., 1992, The Physics of Astrophysics, Volume II, Gas Dynamics, University Science Books, Mill Valley, CA
- Sollins, P., Zhang, Q., Keto, E., Ho, P., 2005, ApJ, 624, L49
- Sollins, P.K., Zhang, Q., Keto, E., Ho, P.T.P., 2005, ApJ, 631, 399
- Spitzer, L., Jr., 1978, Physical Processes in the Interstellar Medium, (New York:Wiley)
- Tan, J.C. & McKee, C.F., 2003, *Star Formation at High Angular Resolution*, ASP Conference Series, Vol S-221, eds: Jayawardhana, R., Burton, M.G., Bourke, T.L., astro-ph/0309139
- Terebey, S., Shu, F., Cassen, P., 1984 ApJ, 286, 529
- Ulrich, R., 1976, ApJ, 210, 377
- Vacca, W.D., Garmany, C.D. & Shull, J.M., 1996, ApJ, 460, 914
- Walmsley, M., 1995, Revista Mexicana de Astronomia y Astrofisica Serie de Conferencias, Vol. 1, Circumstellar Disks, Outflows and Star Formation, Cozumel, Mexico, Nov 28-Dec 2, 1994, p. 137
- Whitney, B.A., Wood, K., Bjorkman, J.E. & Wolff, M.J., 2003, ApJ, 591, 1049
- Wilkin, F.P. & Stahler, S.W., 1998, ApJ, 502, 661

Wood, D.O.S., Wood & Churchwell, E., 1989, *ApJS*, 69, 831

Yorke, H. & Welz, A., 1996, *A&A*, 315, 555

Yorke, H., 1995, *Rev. Mex. AA*, 1, 35

Young, L.M., Keto, E., Ho, P.T.P., 1998, *ApJ*, 507, 270

Zhang, Q. & Ho P., 1997, *ApJ*, 488, 241

Zhang, Q., Hunter, T., Sridharan, T., 1998, *ApJ*, 505, 151

Zhang, Q., Hunter, T., Sridharan, T., Ho, P., 2002, *ApJ*, 566, 982

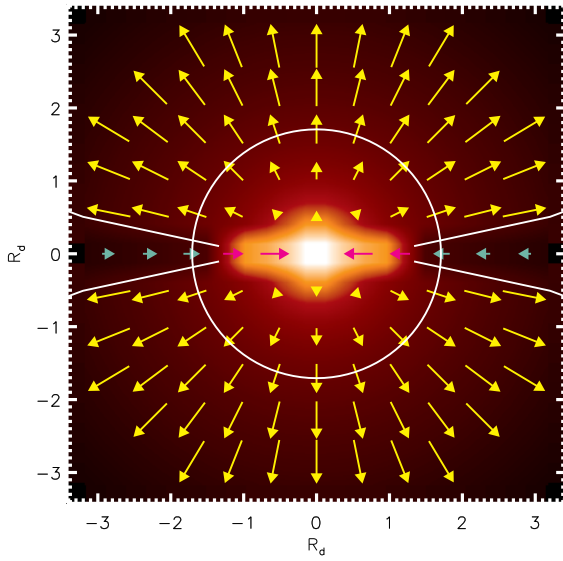
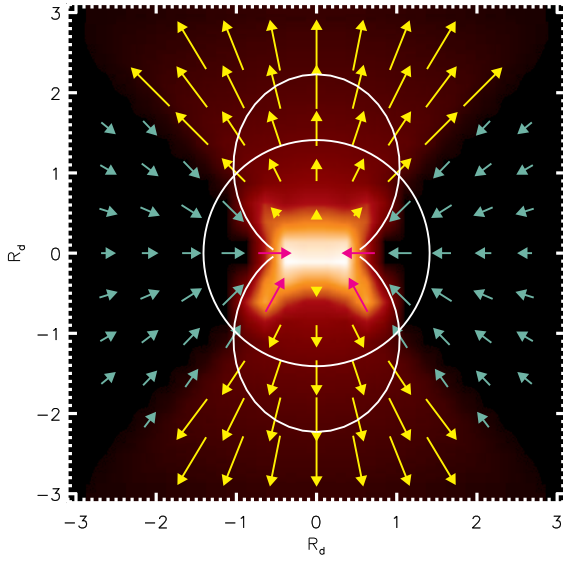
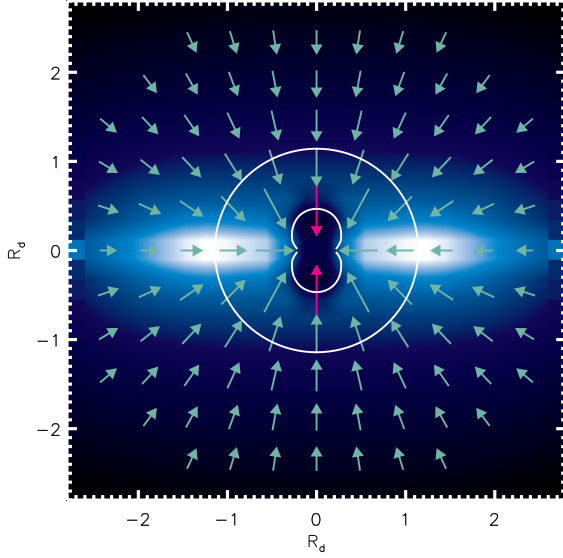




Fig. 1.— Model of a high angular momentum accretion flow subject to 3 levels of ionizing radiation, low (*top*), medium (*medium*), and high (*bottom*) as defined in §6. The figures show the log of the density of molecular gas in blue (*top*) and of the ionized gas in red (*middle* and *bottom*) in a slice in the XZ plane of the flow. The color scales range from 0 to  $1.6 \times 10^7$   $\text{cm}^{-3}$  (molecular) (*top*), from 0 to  $1.2 \times 10^7$   $\text{cm}^{-3}$  (ionized) (*middle*), and 0 to  $1.3 \times 10^7$   $\text{cm}^{-3}$  (ionized) (*bottom*). The circle shows the location of the Bondi-Parker critical radius of the ionized gas for spherical flow. The arrows show the velocity of the flow in the XZ plane. In the top figure, the longest arrow in the molecular flow represents  $26.6 \text{ kms}^{-1}$  and the longest arrow in the ionized flow represents  $21.5 \text{ kms}^{-1}$ . In the middle figure, the longest arrow in the molecular flow represents  $8.0 \text{ kms}^{-1}$  and the longest arrow in the ionized flow represents  $28.2 \text{ kms}^{-1}$ . In the bottom figure, the longest arrow in the molecular flow represents  $5.4 \text{ kms}^{-1}$  and the longest arrow in the ionized flow represents  $29.4 \text{ kms}^{-1}$ . In the ionized outflow flow, the velocity is the sound speed at the critical radius. The axes are labeled in units of  $R_d$ , 42 AU (*left*) and 34 AU (*right*).

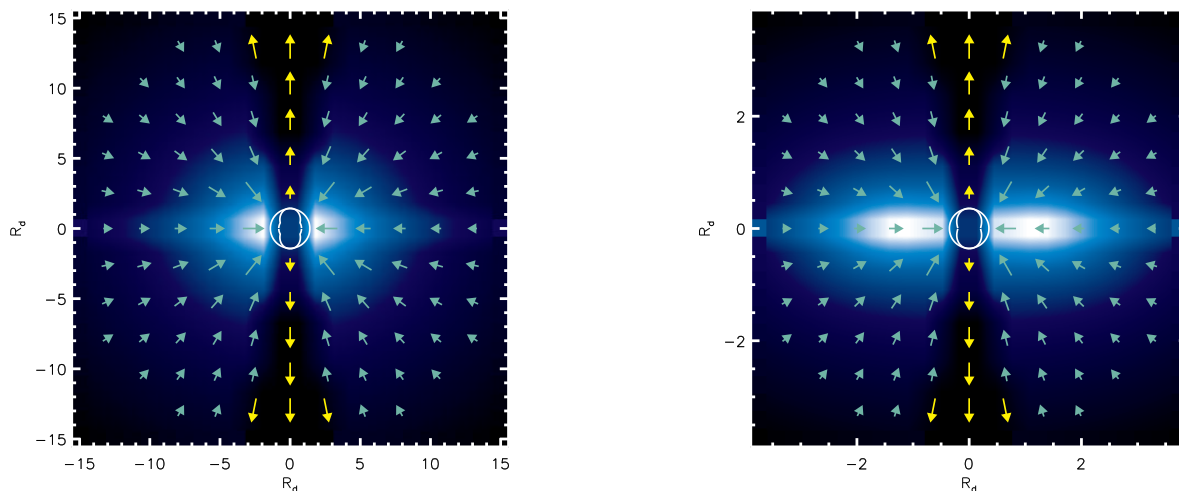


Fig. 2.— Two accretion flows that differ in the relative amount of angular momentum. The flow in the right column has 2 times the angular momentum of the flow in the left column. The two figures show a slice in the XZ plane with the log of the density of the molecular gas in color and the velocity as arrows. The density ranges from  $4.5 \times 10^3$  to  $4.5 \times 10^6 \text{ cm}^{-3}$  (molecular) (*left*) and from  $4.5 \times 10^3$  to  $5.2 \times 10^6 \text{ cm}^{-3}$  (*right*). The longest arrow in the molecular flow (blue arrows) represents  $1.8 \text{ km s}^{-1}$  (*left*) and  $0.4 \text{ km s}^{-1}$  (*right*). The yellow arrows show the velocity of the ionized outflow at half the scale.